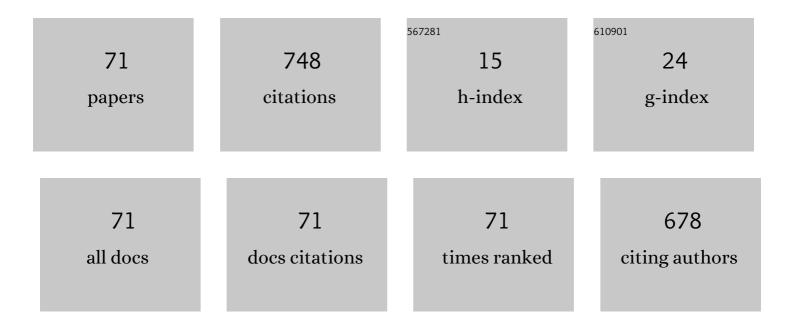
Renata Ratajczak

List of Publications by Year in descending order

Source: https://exaly.com/author-pdf/1723139/publications.pdf Version: 2024-02-01



#	Article	IF	CITATIONS
1	Modern analysis of ion channeling data by Monte Carlo simulations. Nuclear Instruments & Methods in Physics Research B, 2005, 240, 277-282.	1.4	108
2	Hydrogen release in UHMWPE upon He-ion bombardment. Vacuum, 2005, 78, 281-284.	3.5	58
3	Mechanism of damage buildup in ion bombarded ZnO. Acta Materialia, 2017, 134, 249-256.	7.9	56
4	Ni-Based Ohmic Contacts to <i>n</i> -Type 4H-SiC: The Formation Mechanism and Thermal Stability. Advances in Condensed Matter Physics, 2016, 2016, 1-26.	1.1	41
5	Long-term stability of Ni–silicide ohmic contact to n-type 4H–SiC. Microelectronic Engineering, 2008, 85, 2142-2145.	2.4	25
6	Fabrication and characterization of nickel silicide ohmic contacts to n-type 4H silicon carbide. Journal of Physics: Conference Series, 2008, 100, 042003.	0.4	24
7	The photoluminescence response to structural changes of Yb implanted ZnO crystals subjected to non-equilibrium processing. Journal of Applied Physics, 2017, 121, .	2.5	23
8	Monte Carlo simulations of ion channeling in crystals containing dislocations and randomly displaced atoms. Journal of Applied Physics, 2019, 126, .	2.5	21
9	On the Formation of Ni-Based Ohmic Contacts to n-Type 4H-SiC. Materials Science Forum, 2009, 615-617, 573-576.	0.3	19
10	RBS/Channeling and TEM Study of Damage Buildup in Ion Bombarded GaN. Acta Physica Polonica A, 2011, 120, 153-155.	0.5	18
11	Virtues and pitfalls in structural analysis of compound semiconductors by the complementary use of RBS/channeling and high resolution X-ray diffraction. Nuclear Instruments & Methods in Physics Research B, 2004, 219-220, 618-625.	1.4	17
12	Modification of UHMWPE by ion, electron and \hat{I}^3 -ray irradiation. Vacuum, 2009, 83, S54-S56.	3.5	17
13	Nanoscale Electrostructural Characterization of Compositionally Graded Al _{<i>x</i>} Ga _{1–<i>x</i>} N Heterostructures on GaN/Sapphire (0001) Substrate. ACS Applied Materials & Interfaces, 2015, 7, 23320-23327.	8.0	17
14	RBS/C, XRR, and XRD Studies of Damage Buildup in Erâ€Implanted ZnO. Physica Status Solidi (B): Basic Research, 2019, 256, 1800364.	1.5	17
15	Thermal degradation of Au/Ni2Si/n-SiC ohmic contacts under different conditions. Materials Science and Engineering B: Solid-State Materials for Advanced Technology, 2009, 165, 38-41.	3.5	16
16	Atomic layer deposited ZnO films implanted with Yb: The influence of Yb location on optical and electrical properties. Thin Solid Films, 2017, 643, 7-15.	1.8	16
17	Amorphous Ta–Si–N diffusion barriers on GaAs. Thin Solid Films, 2004, 459, 292-296.	1.8	14
18	Compositional dependence of damage buildup in Ar-ion bombarded AlGaN. Vacuum, 2009, 83, S145-S147.	3.5	14

Renata Ratajczak

#	Article	IF	CITATIONS
19	Hydrogen-ion implantation in GaAs. Vacuum, 2001, 63, 697-700.	3.5	12
20	Comparative study of radiation-induced damage in magnesium aluminate spinel by means of IL, CL and RBS/C techniques. Physics and Chemistry of Minerals, 2016, 43, 439-445.	0.8	12
21	Structural and optical studies of Pr implanted ZnO films subjected to a long-time or ultra-fast thermal annealing. Thin Solid Films, 2017, 643, 24-30.	1.8	11
22	Luminescence in the Visible Region from Annealed Thin ALDâ€ZnO Films Implanted with Different Rare Earth Ions. Physica Status Solidi (A) Applications and Materials Science, 2018, 215, 1700889.	1.8	11
23	Correlations between the structural transformations and concentration quenching effect for RE-implanted ZnO systems. Applied Surface Science, 2020, 521, 146421.	6.1	10
24	Defect evolution in Ni and solid-solution alloys of NiFe and NiFeCoCr under ion irradiation at 16 and 300ÂK. Journal of Nuclear Materials, 2020, 534, 152138.	2.7	10
25	Resonant Photoemission Spectroscopy Study on the Contribution of the Yb 4f States to the Electronic Structure of ZnO. Acta Physica Polonica A, 2018, 133, 907-909.	0.5	9
26	Barrier properties of Ta–Si–N films in Ag-and Au-containing metallization. Vacuum, 2004, 74, 195-199.	3.5	8
27	Structural and tribological properties of carbon steels modified by plasma pulses containing inert and active ions. Surface and Coatings Technology, 2007, 201, 8295-8298.	4.8	8
28	Electron-beam pulse annealed Ti-implanted GaP. Journal of Applied Physics, 2016, 120, 085103.	2.5	8
29	Stopping Power and Energy Straggling of Channeled He-Ions in GaN. Acta Physica Polonica A, 2011, 120, 163-166.	0.5	8
30	Characterization of InGaN/GaN heterostructures by means of RBS/channeling. Nuclear Instruments & Methods in Physics Research B, 2000, 161-163, 539-543.	1.4	7
31	Ion Beam Modification of ZnO Epilayers: Sequential Processing. Physica Status Solidi (A) Applications and Materials Science, 2018, 215, 1700887.	1.8	7
32	Modification of the near surface layer of carbon steels with intense argon and nitrogen plasma pulses. Vacuum, 2005, 78, 181-186.	3.5	6
33	Relationship between Condition of Deposition and Properties of W-Ti-N Thin Films Prepared by Reactive Magnetron Sputtering. Advanced Engineering Materials, 2006, 8, 209-212.	3.5	6
34	Luminescence analysis of damage accumulation; case study of calcium molybdate. Nuclear Instruments & Methods in Physics Research B, 2014, 332, 60-62.	1.4	6
35	Electrical properties of ZnO films implanted with rare earth and their relationship with structural and optical parameters. Materials Science and Engineering B: Solid-State Materials for Advanced Technology, 2022, 275, 115526.	3.5	6
36	Nitrogen sublattice analysis in GaN by non-Rutherford He-ion scattering. Nuclear Instruments & Methods in Physics Research B, 2008, 266, 1897-1902.	1.4	5

Renata Ratajczak

#	Article	IF	CITATIONS
37	Reliability Tests of Au-Metallized Ni-Based Ohmic Contacts to 4H-n-SiC with and without Nanocomposite Diffusion Barriers. Materials Science Forum, 0, 645-648, 737-740.	0.3	5
38	Comparison of the structural properties of Zn-face and O-face single crystal homoepitaxial ZnO epilayers grown by RF-magnetron sputtering. Journal of Applied Physics, 2017, 121, .	2.5	5
39	Determination of hydrogen in GaMnN and GaMnMgN by nuclear reaction analysis. Vacuum, 2003, 70, 207-213.	3.5	4
40	Thermal stability of the phases formed in the near surface layers of unalloyed steels by nitrogen pulsed plasma treatment. Vacuum, 2007, 81, 1188-1190.	3.5	4
41	Channeling study of thermal decomposition of III-N compound semiconductors. Nuclear Instruments & Methods in Physics Research B, 2008, 266, 1224-1228.	1.4	4
42	Strain profiles and defect structure in 6H–SiC crystals implanted with 2MeV As+ ions. Vacuum, 2009, 83, S40-S44.	3.5	4
43	Chemical effects in Zr- and Co-implanted sapphire. Vacuum, 2009, 83, S57-S60.	3.5	4
44	RBS/Channeling Analysis of Zinc Oxide Films Grown at Low Temperature by Atomic Layer Deposition. Acta Physica Polonica A, 2013, 123, 899-903.	0.5	4
45	Ion beam-induced luminescence as method of characterization of radiation damage in polycrystalline materials. Nuclear Instruments & Methods in Physics Research B, 2015, 365, 273-277.	1.4	4
46	Valence band of ZnO:Yb probed by resonant photoemission spectroscopy. Materials Science in Semiconductor Processing, 2019, 91, 306-309.	4.0	4
47	Optical Response of Epitaxial ZnO Films Grown by Atomic Layer Deposition and Coimplanted with Dy and Yb. Physica Status Solidi (B): Basic Research, 2020, 257, 1900513.	1.5	4
48	On the Question of Ferromagnetism in Proton and He-Irradiated Carbon. Acta Physica Polonica A, 2008, 114, 1387-1390.	0.5	4
49	Damage buildup and recovery in III–V compound semiconductors at low temperatures. Nuclear Instruments & Methods in Physics Research B, 2005, 240, 105-110.	1.4	3
50	Towards identification of localized donor states in InN. Semiconductor Science and Technology, 2007, 22, 1161-1164.	2.0	3
51	Phase Composition and Properties of Unalloyed Steels' Surfaces Modified by Intense Plasma Pulses with Various Reactive Gas Fluencies. Plasma Processes and Polymers, 2007, 4, S314-S318.	3.0	3
52	Proton beam induced luminescence of silicon dioxide implanted with silicon. Nuclear Instruments & Methods in Physics Research B, 2009, 267, 2579-2582.	1.4	3
53	Advanced Monte Carlo Simulations for Ion-Channeling Studies of Complex Defects in Crystals. Springer Series in Materials Science, 2020, , 133-160.	0.6	3
54	Structural analysis of distributed Bragg reflector mirrors. Vacuum, 2009, 83, S148-S151.	3.5	2

ΓΕΝΑΤΑ ΚΑΤΑΙCZAK

#	Article	IF	CITATIONS
55	Channeled PIXE and magnetic measurements in Co implanted and thermally annealed ZnO single crystals. Applied Surface Science, 2014, 310, 242-247.	6.1	2
56	lon implantation of the <scp>4H SiC</scp> epitaxial layers and substrates with 2 <scp>MeV Se⁺</scp> and 1 <scp>MeV Al⁺</scp> ions. X-Ray Spectrometry, 2015, 44, 371-3	378 ^{1.4}	2
57	Stoichiometric MgB2 layers produced by multi-energy implantation of boron into magnesium. Surface and Coatings Technology, 2009, 203, 2712-2716.	4.8	1
58	Stability of gold bonding and Ti/Au ohmic contact metallization to n-SiC in high power devices. , 2009, , .		1
59	Low energy cathodoluminescence analysis of damage build-up in ion irradiated spinel mono- and polycrystals. Nuclear Instruments & Methods in Physics Research B, 2018, 435, 290-295.	1.4	1
60	Defect Transformations in Ion Bombarded InGaAsP. Acta Physica Polonica A, 2011, 120, 136-139.	0.5	1
61	Channeling Study of Co and Mn Implanted and Thermally Annealed Wide Band-Gap Semiconducting Compounds. Acta Physica Polonica A, 2015, 128, 845-849.	0.5	1
62	Polarized dependence of soft X-ray absorption near edge structure of ZnO films implanted by Yb. Materials Science in Semiconductor Processing, 2022, 144, 106609.	4.0	1
63	<title>AgTe/ZrB<formula><inf><roman>2</roman></inf></formula>/Au multilayer metallization for
improved ohmic contacts to n-GaSb</title> . , 2003, , .		0
64	Characterization of the near-surface layers of carbon steels modified by interaction with intense pulsed plasma beams: scanning electron microscopy investigations. Journal of Microscopy, 2006, 224, 114-116.	1.8	0
65	Structural Characterization of GaN Epitaxial Layers Grown on 4H-SiC Substrates with Different Off-Cut. Materials Science Forum, 2009, 615-617, 939-942.	0.3	0
66	Cathodoluminescence-Based Quantitative Analysis of Radiation Damage in Powellite Single Crystals. Microscopy and Microanalysis, 2013, 19, 1108-1109.	0.4	0
67	Analysis of Radiation Damage in Magnesium Aluminate Spinel by Means of Cathodoluminescence. Microscopy and Microanalysis, 2015, 21, 1005-1006.	0.4	0
68	The stopping power of heavy ions for energies below 0.2 MeV/nucleon measured by the semi-thick target method. Nuclear Instruments and Methods in Physics Research, Section A: Accelerators, Spectrometers, Detectors and Associated Equipment, 2015, 774, 82-88.	1.6	0
69	Effect of rapid thermal annealing on damage of silicon matrix implanted by low-energy rhenium ions. Journal of Alloys and Compounds, 2020, 846, 156433.	5.5	0
70	Post-implantation defects in heavy ion implanted monocrystalline ZnO. Radiation Effects and Defects in Solids, 0, , 1-11.	1.2	0
71	Electron Microscopy and X-ray Diffraction Study of AlN Layers. Acta Physica Polonica A, 2002, 102, 221-225.	0.5	Ο